Featured Article

Genome-wide association analysis of dementia and its clinical endophenotypes reveal novel loci associated with Alzheimer's disease and three causality networks: The GR@ACE project

Sonia Moreno-Grau[a,b], Itziar de Rojas[a], Isabel Hernández[a,b], Inés Quintela[c], Laura Montrreal[a], Montserrat Alegret[a,b], Begoña Hernández-Olasagarre[a], Laura Madrid[d], Antonio González-Perez[d], Olalla Maroñas[c], Maitée Rosende-Roca[a], Ana Mauleón[a], Liliana Vargas[a], Asunción Lafuente[a], Carla Abdelnour[a,b], Octavio Rodríguez-Gómez[a,b], Silvia Gil[a], Miguel Ángel Santos-Santos[a], Ana Espinosa[a,b], Gemma Ortega[a,b], Ángela Sanabria[a,b], Alba Pérez-Cordón[a], Pilar Cañabate[a,b], Mariola Moreno[a], Silvia Preckler[a], Susana Ruiz[a,b], Nuria Aguilera[a], Juan Antonio Pineda[e], Juan Macías[e], Emilio Alarcón-Martín[a,f], Oscar Sotolongo-Grau[a], GR@ACE consortium[**], DEGESCO consortium[**], Alzheimer's Disease Neuroimaging Initiative, Marta Marquié[a], Gemma Monté-Rubio[a], Sergi Valero[a,b], Alba Benaque[a], Jordi Clarimón[b,g], Maria Jesus Bullido[b,h,i], Guillermo García-Ribas[j], Pau Pástor[k], Pascual Sánchez-Juan[b,l], Victoria Álvarez[m,n], Gerard Piñol-Ripoll[b,o], Jose Maria García-Alberca[p], José Luis Royo[f], Emilio Franco[q], Pablo Mir[b,r], Miguel Calero[b,s,t], Miguel Medina[b,s], Alberto Rábano[b,s,u], Jesús Ávila[b,v], Carmen Antúnez[w], Luis Miguel Real[e,f], Adelina Orellana[a], Ángel Carracedo[c,x], María Eugenia Sáez[d], Lluís Tárraga[a,b], Mercè Boada[a,b], Agustín Ruiz[a,b,*]

[a]Research Center and Memory clinic Fundació ACE, Institut Català de Neurociències Aplicades, Universitat Internacional de Catalunya, Barcelona, Spain
[b]CIBERNED, Network Center for Biomedical Research in Neurodegenerative Diseases, National Institute of Health Carlos III, Madrid, Spain
[c]Grupo de Medicina Xenómica, Centro Nacional de Genotipado (CEGEN-PRB3-ISCIII). Universidade de Santiago de Compostela, Santiago de Compostela, Spain
[d]CAEBI, Centro Andaluz de Estudios Bioinformáticos, Sevilla, Spain
[e]Unidad Clínica de Enfermedades Infecciosas y Microbiología. Hospital Universitario de Valme, Sevilla, Spain
[f]Department of Surgery, Biochemistry and Molecular Biology, School of Medicine, University of Málaga, Málaga, Spain
[g]Memory Unit, Neurology Department and Sant Pau Biomedical Research Institute, Hospital de la Santa Creu i Sant Pau, Universitat Autònoma de Barcelona, Barcelona, Spain
[h]Centro de Biologia Molecular Severo Ochoa (C.S.I.C.-U.A.M.), Universidad Autonoma de Madrid, Madrid, Spain
[i]Instituto de Investigacion Sanitaria "Hospital la Paz" (IdIPaz), Madrid, Spain
[j]Hospital Universitario Ramón y Cajal, Madrid, Spain
[k]Fundació per la Recerca Biomèdica i Social Mútua Terrassa, and Memory Disorders Unit, Department of Neurology, Hospital Universitari Mutua de Terrassa, University of Barcelona School of Medicine, Terrassa, Spain
[l]Neurology Service 'Marqués de Valdecilla' University Hospital (University of Cantabria and IDIVAL), Santander, Spain
[m]Laboratorio de Genética Hospital Universitario Central de Asturias, Oviedo, Spain
[n]Instituto de Investigación Biosanitaria del Principado de Asturias (ISPA), Oviedo, Spain
[o]Unitat Trastorns Cognitius, Hospital Universitari Santa Maria de Lleida, Institut de Recerca Biomédica de Lleida (IRBLLeida), Lleida, Spain

*Corresponding author. Tel: +3493.444.73.18; Fax: +3493.410.17.01.
E-mail address: aruiz@fundacioace.org

[p]Alzheimer Research Center & Memory Clinic, Andalusian Institute for Neuroscience, Málaga, Spain
[q]Unidad de Demencias, Servicio de Neurología y Neurofisiología. Instituto de Biomedicina de Sevilla (IBiS), Hospital Universitario Virgen del Rocío/CSIC/Universidad de Sevilla, Seville, Spain
[r]Unidad de Trastornos del Movimiento, Servicio de Neurología y Neurofisiología. Instituto de Biomedicina de Sevilla (IBiS), Hospital Universitario Virgen del Rocío/CSIC/Universidad de Sevilla, Seville, Spain
[s]CIEN Foundation, Queen Sofia Foundation Alzheimer Center, Madrid, Spain
[t]Instituto de Salud Carlos III (ISCIII), Madrid, Spain
[u]BT-CIEN, Madrid, Spain
[v]Department of Molecular Neuropathology, Centro de Biología Molecular "Severo Ochoa" (CBMSO), Consejo Superior de Investigaciones Científicas (CSIC)/Universidad Autónoma de Madrid (UAM), Madrid, Spain
[w]Unidad de Demencias, Hospital Clínico Universitario Virgen de la Arrixaca, Murcia, Spain
[x]Fundación Pública Galega de Medicina Xenómica- CIBERER-IDIS, Santiago de Compostela, Spain

Abstract

Introduction: Large variability among Alzheimer's disease (AD) cases might impact genetic discoveries and complicate dissection of underlying biological pathways.

Methods: Genome Research at Fundacio ACE (GR@ACE) is a genome-wide study of dementia and its clinical endophenotypes, defined based on AD's clinical certainty and vascular burden. We assessed the impact of known AD loci across endophenotypes to generate loci categories. We incorporated gene coexpression data and conducted pathway analysis per category. Finally, to evaluate the effect of heterogeneity in genetic studies, GR@ACE series were meta-analyzed with additional genome-wide association study data sets.

Results: We classified known AD loci into three categories, which might reflect the disease clinical heterogeneity. Vascular processes were only detected as a causal mechanism in probable AD. The meta-analysis strategy revealed the *ANKRD31*-rs4704171 and *NDUFAF6*-rs10098778 and confirmed *SCIMP*-rs7225151 and *CD33*-rs3865444.

Discussion: The regulation of vasculature is a prominent causal component of probable AD. GR@ACE meta-analysis revealed novel AD genetic signals, strongly driven by the presence of clinical heterogeneity in the AD series.

© 2019 The Authors. Published by Elsevier Inc. on behalf of the Alzheimer's Association. This is an open access article under the CC BY-NC-ND license (http://creativecommons.org/licenses/by-nc-nd/4.0/).

Keywords:　　Alzheimer's disease; Vascular pathology; Cerebral amyloid angiopathy; GWAS; Biological pathway

1. Background

Dementia is an age-related clinical syndrome that devastates cognitive abilities and interferes in elderly people's daily activities. Although its incidence is decreasing due to improvements to public health systems and control of cardiovascular risk factors [1], its prevalence is steadily increasing due to rising life expectancy of human populations [2].

Dementia is linked to many underlying pathologies, with Alzheimer's disease (AD) being the most common condition. Clinical AD is a heterogeneous syndrome. Brain autopsies have shown that roughly 80% of clinical AD patients present with brain vascular pathology [3] in addition to the common neuropathological AD hallmarks: amyloidosis, neurofibrillary tangles, and cerebral amyloid angiopathy (CAA) [4]. In fact, brain vascular pathology has been shown to be an important risk factor for AD that accelerates cognitive decline [5] and lowers the threshold for clinical diagnosis of AD [6]. In that context, it has been suggested that dementia is represented by a gradient of neurodegenerative and vascular components [7], from pure AD forms, with a strong neurodegenerative component, to pure vascular dementia (VaD) cases and in-between mixed pathologies,

representing the coexistence of both neurodegenerative and vascular components [7]. Despite that, whether there are differential biological routes operating under different levels of vascular burden in clinical AD patients remains mostly unknown.

In the search for the etiology of AD, genetic factors play a pivotal role. Two forms of the disease can be differentiated according to individual genetic background. The Mendelian form is an uncommon disorder that mainly affects families with early-onset AD (<65 years), whereas the polygenic form is a complex disorder mainly appearing in sporadic cases with late-onset AD (LOAD) (>65 years). Highly penetrant mutations detected in families with early-onset AD have been pinpointed to three genes: *APP* [8], *PSEN1* [9], and *PSEN2* [10], leading to the establishment of the amyloid hypothesis as a potential causal mechanism for the disease [11].

LOAD heritability falls in the range of 13%–80% [12,13]. Although *APOE* ε4 was the first to be discovered and still remains the strongest genetic risk factor for AD [14], almost 40 additional genetic variants have been identified [15–17] using genome-wide association studies (GWAS) and large

sequencing projects. Among the biological pathways underlying genetic hits, the roles of the immune system, cholesterol, amyloid, and tau metabolism have been highlighted [18]. Despite these, current genetic findings account for 31% of LOAD heritability [19], and the biological picture of AD is still poorly understood. Several reasons can explain this. Among them, the presence of clinical and neuropathological heterogeneity between AD cases in genetic studies, as recently demonstrated [12], might compromise the power to detect genuine genetic associations and decrease the estimates of risk attributed to genetic variation.

The neuropathological variability in clinical AD cases comprises a wide spectrum, from those with concomitant vascular brain disease to those with a pure AD phenotype, as previously proposed by Viswanathan et al. [7]. This large heterogeneity might hamper the identification of functional categories of genes underlying differential biological routes to dementia and might impact AD genetic studies. To gain insight into the causality networks behind AD clinical subgroups and to explore their impact in large GWAS, we conducted the Genome Research at Fundacio ACE (GR@ACE) study. This is a GWAS of dementia and its clinical endophenotypes defined based on AD's clinical certainty and the burden of vascular comorbidity. The GR@ACE is a unique genomic resource comprising the largest number of dementia cases diagnosed in a single memory clinic to date. First, we determined whether we could identify categories of known LOAD genes linked to clinical subgroups of AD cases. Next, we explored whether these categories suggested different biological routes. Finally, to assess the impact of these clinical subgroups of AD cases in GWAS findings, we meta-analyzed the GR@ACE data with independent GWAS series.

2. Methods

2.1. Subjects

2.1.1. GR@ACE cohort and phenotype definitions

The GR@ACE study comprises 4120 AD cases and 3289 control individuals (Table 1). Cases were recruited from Fundació ACE, Institut Català de Neurociències Aplicades (Catalonia, Spain). Diagnoses were established by a multidisciplinary working group, including neurologists, neuropsychologists, and social workers, according to the Diagnostic and Statistical Manual of Mental Disorders–IV criteria for dementia and to the National Institute on Aging and Alzheimer's Association's (NIA-AA) 2011 guidelines for defining AD [20] (see Supplementary Material). In the present study, we considered AD cases as dementia individuals diagnosed with probable or possible AD at any moment of their clinical course.

We took advantage of this wide clinical definition to refine AD cases. Considering the dementia spectrum proposed by Viswanathan et al. [7], we classified Gr@ACE AD patients according to the degree of clinical certainty for AD phenotype and the presence of vascular comorbidity, from "pure" clinical AD cases to mixed and vascular en-

riched cases. This approach was feasible due to Fundació ACE's endorsement of a primary and a secondary etiologic diagnosis as well as routine follow-up evaluations [21] (Supplementary Methods). Using the entire clinical chart of each subject, we differentiated five clinical subgroups of patients representing the GR@ACE endophenotypes: (1) the AD^{+++} endophenotype comprises individuals with a last clinical diagnosis of probable AD in both primary and secondary diagnoses (n = 1854); (2) the AD^{++} includes individuals diagnosed with probable AD in the primary diagnosis and probable or possible AD in the secondary diagnosis (n = 2611); (3) the AD^{+} encompasses patients diagnosed with probable or possible AD either in the primary diagnosis or in the secondary diagnosis (n = 3797); (4) the VaD^{+} includes patients diagnosed with VaD or possible AD in the primary diagnosis (n = 1168); and (5) the VaD^{++} comprises patients diagnosed with probable or possible vascular dementia in the primary diagnosis (n = 373) (Table 1) (Supplementary Fig. 1). Patients with VaD were defined according to the Neuroepidemiology Branch of the National Institute of Neurological Disorders and Stroke and the Association Internationale pour la Recherche et l'Enseignement en Neurosciences criteria [22].

Control individuals were recruited from three centers: Fundació ACE (Barcelona, Spain), Valme University Hospital (Seville, Spain), and the Spanish National DNA Bank Carlos III (University of Salamanca, Spain) (www.bancoadn.org). Written informed consent was obtained from all participants. The Ethics and Scientific Committees have approved this research protocol (Acta 25/2016. Ethics Committee. H. Clinic i Provincial, Barcelona, Spain).

2.1.2. Replication sample

With the objective to successfully replicate novel GWAS findings, we used an independent Spanish sample of 1943 AD cases (mean age = 79.2; standard deviation [SD] = 7.6; 66.3% women) and 3016 controls (mean age = 52.8; SD = 15.2; 46% women) presenting similar characteristics to the GR@ACE cohort and with available genetic data. All AD cases were examined at a single site, Fundació ACE, Institut Català de Neurociències Aplicades (Catalonia, Spain), and were assessed by applying the same criteria previously explained. The sample composition of dementia cases comprised 30.1% of AD^{+++} (n = 584), 53.9% of AD^{++} (n = 1048), 91.9% of AD^{+} (n = 1783), 23.0% of VaD^{+} (n = 447), and 4.6% of VaD^{++} (n = 89) cases. Control individuals were selected from the Spanish population available at three centers, previously described.

2.2. GWAS genotyping, quality control, imputation, and statistical analysis

Participants were genotyped using the Axiom 815K Spanish Biobank Array (Thermo Fisher). Genotyping was performed in the Spanish National Center for Genotyping

Table 1
GR@ACE demographic characteristics and endophenotype definitions

Phenotype	Primary diagnostic	Secondary diagnostic	N	Mean age ± SD	Women %	APOE ε4 %
Controls	–	–	3289	54.3 ± 14.4	48.9	21.4
VaD^{++}	VaD	Pss AD	373	80.1 ± 5.5	54.9	25.0
VaD^{+}	VaD/Pss AD	VaD/Pss AD	1168	80.4 ± 6.3	65.0	32.8
AD	Pr/Pss AD at any time in medical history		4120	79.0 ± 7.5	69.6	40.1
AD^{+}	Pr/Pss AD	Pr/Pss AD	3797	79.2 ± 7.5	70.6	41.2
AD^{++}	Pr AD	Pr/Pss AD	2611	78.8 ± 7.9	72.8	44.6
AD^{+++}	Pr AD	Pr AD	1854	79.0 ± 8.0	74.6	47.0

Abbreviations: AD, Alzheimer's disease; SD, standard deviation; VaD, vascular dementia; Pss AD, possible AD; Pr AD, probable AD.

(CeGEN, Santiago de Compostela, Spain) (Supplementary Methods).

We removed samples with genotype call rates <97%, excess heterozygosity, duplicates, samples genetically related to other individuals in the cohort, or sample mix-up (PIHAT >0.1875). If a sex discrepancy was detected, the sample was removed unless the discrepancy was safely resolved. To detect population outliers of non-European ancestry (>6 SD from European population mean), principal component analysis was conducted using SMARTPCA from EIGENSOFT 6.1.4 (Fig. 1) (Supplementary Methods).

We excluded variants with a call rate <95% or that grossly deviated from Hardy-Weinberg equilibrium in controls (P value $\leq 1 \times 10^{-6}$); we also excluded markers with a different missing rate between case and control (P value $< 5 \times 10^{-4}$ for the difference) or a minor allele frequency (MAF) < 0.01. Imputation was carried out using the Haplotype Reference Consortium panel in the Michigan Imputation Server (https://imputationserver.sph.umich.edu). Only common markers (MAF >0.01) with a high imputation quality ($R^2 > 0.30$) were selected for downstream analyses.

The GWAS was performed for GR@ACE as a whole and for each endophenotype, ([N $_{AD+++}$ = 5143]; [N $_{AD++}$ = 5900]; [N $_{AD+}$ = 7086]; [N $_{AD}$ $_{dementia}$ = 7409]; [N $_{VaD+}$ = 4487]; and [N $_{VaD++}$ = 3662]). The GWAS was conducted for genotype dosages using an additive genetic model with PLINK 1.9. A model including the top four PCs as covariates was used for the discovery stage because it exhibited the lowest inflation and optimal power compared with alternative tested models (Supplementary Fig. 2). Further description is provided in Supplementary Methods. Power analysis was performed using QUANTO software v1.2.4 [23] to model the impact on statistical power at different MAFs and effect sizes in available case-control cohorts. Results were depicted using the ggplot2 package in R. Analyses were performed for a GWAS experiment that would meet criteria for genome-wide significance ($P < 5 \times 10^{-8}$) and for a replication experiment that would meet $P < .05$ (Supplementary Fig. 3). Calculations were performed considering a disease prevalence of 1.73%, according to registers in the Spanish population.

GR@ACE GWAS data have been deposited into the European Genome-phenome Archive (https://ega-archive.org), which is hosted by the European Bioinformatics Institute and the Center for Genomic Regulation, under the accession number EGAS00001003424.

2.3. Genetic exploration of GR@ACE clinical endophenotypes and enrichment analysis

With the objective to explore whether different biological routes operate under different levels of vascular burden in clinical AD patients, first, we classified GR@ACE dementia cases to cover the dementia spectrum previously proposed by Viswanathan et al. [7] (see Section 2.1). Second, we extracted the effect (odds ratio [OR]) for known LOAD genetic variants (MAF >1%). See included variants in Supplementary Table 1. Then, we explored whether previously identified LOAD variants were more strongly associated with a specific subgroup of AD patients. We quantified the strength of the association for each variant across endophenotypes, named henceforth global effect change. It was calculated as the absolute difference between variant OR for extreme endophenotypes (VaD^{++} vs. AD^{+++}). According to the global effect change and direction of the enrichment, i.e., from VaD^{++} to AD^{+++} or from AD^{+++} to VaD^{++}, we classified LOAD genetic variants into three categories. Thus, category A includes variants with an increase in the association effect from VaD^{++} to AD^{+++} endophenotypes and a global effect change >0.05, and category B includes variants with an increase in the association effect from AD^{+++} to VaD^{++} and a global effect change >0.05. Category C comprises variants not fulfilling criteria for categories A or B (Supplementary Table 1). Finally, we assessed the biological pathways underlying each category. We incorporated data from gene co-expression for each specific gene category using the GeneFriends tool (http://genefriends.org/) and performed pathway analysis of top coexpressed genes using the over-representation enrichment method in WebGestalt (http://www.webgestalt.org/option.php) (see Supplementary Methods). With the objective to further explore potential additional trends in category C, we performed a specific subanalysis in this category, widely described in Supplementary Methods. To validate previous gene classification, which
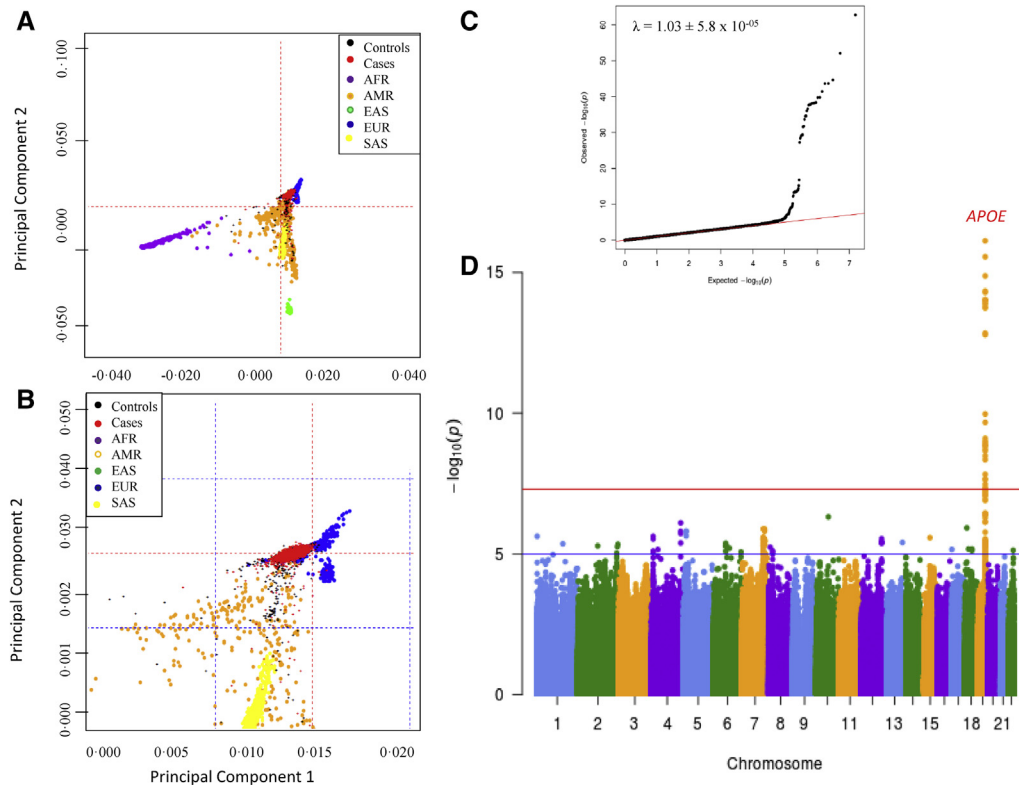
Fig. 1. Results of genome-wide association analysis for the GR@ACE data set (n = 7409). (A) Principal component analysis; (B) principal component analysis centered in European population; (C) QQplot for the discovery model, adjusted for first four PCs; (D) Manhattan plot for genome-wide results. Abbreviations: AFR, African; AMR, Admixed American; EAS, East Asian; EUR, European; SAS, South Asian.

strongly determines the pathway analysis results, we conducted a stringent subanalysis (see Supplementary Methods and Supplementary Fig. 4).

2.4. Meta-analysis: Data sets and association analysis

To explore the impact of the different clinical endophenotypes in GWAS findings, we combined the whole GR@ACE GWAS data set, which represents a dementia set of samples and its endophenotypes with (1) genotype-level data from nine additional GWAS series (N = 13,826), available through dbGaP (https://www.ncbi.nlm.nih.gov/gap) that we processed by applying identical quality control and imputation procedures to those described for the GR@ACE cohort (Supplementary Table 2) and (2) aggregated summary statistics available from the International Genomics Alzheimer's Project (IGAP) (http://web.pasteur-lille.fr/en/recherche/u744/igap/igap_download.php) [24], including IGAP stages I (N final = 61,571) and IGAP I and II (N final = 81,455) (Supplementary Methods). Meta-analyses were conducted using the inverse variant method in METAL software (https://genome.sph.umich.edu/wiki/METAL). The linkage disequilibrium (LD) score calculations, clumping, and conditional analysis are described in Supplementary Methods.

2.5. Replication of genome-wide significant findings

We then explored genome-wide significant (GWS) signals in an independent cohort of Spanish ancestry (N = 4959). We extracted variants of interest from GWAS data, which were genotyped and processed applying similar methods to those explained for the GR@ACE study (Section 2.3). Finally, meta-analysis including the discovery stage, named stage I, and the replica data set, stage II, was performed as previously described. Results were interpreted according to the American Statistical Association guidelines [25,26].

2.6. Biological interpretation of meta-GWAS signals

Gene expression quantitative trait locus (eQTL) analysis was conducted to link meta-GWAS top signals to genes. Markers with moderate-to-high LD ($r^2 \geq 0.6$) with the novel lead markers were identified using LDlink [27] for European population and were included in this analysis. We used brain (n = 11) and whole-blood (n = 1) tissues from the GTEx v7 repository (https://www.gtexportal.org/home) for mapping cis-eQTLs (Supplementary Table 3). As an extension of GTEx tissue eQTL mapping, we explored brain eQTLs for GWS genomic regions using additional databases available via Functional Mapping and Annotation of Genome-Wide Association Studies (FUMA) [28]. We also performed

functional annotation for GWS markers, chromatin interaction, and gene-based analysis using similar criteria to those previously described by Jansen et al. [17] (see Supplementary Methods).

3. Results

3.1. GR@ACE genome-wide association study

After quality control and imputation, the GR@ACE study encompassed 7409 unrelated individuals from the Spanish population and 7.7 million variants (λ_{GC} = 1.03). The *APOE*-rs429358 marker was the only one to have a GWS association (OR = 2.27 [2.06–2.50]; $P = 1.25 \times 10^{-62}$) (Fig. 1). Four additional LOAD variants displayed statistically significant evidence of replication (*BIN1*-rs6733839, *MAPT*-rs2732703, *MS4A2*-rs983392, and *PICALM*-rs10792832) and nine additional markers presented a consistent direction for the effect (Supplementary Table 1). *MAPT* marker association remains significant in *APOE* ε4 noncarriers, but the effect size was stable in both strata (Supplementary Table 4). GWAS of clinical endophenotypes showed that *CNTNAP2*-rs117834366 was associated with the VaD^{++} endophenotype (Table 2). This marker is in complete linkage equilibrium with *CNTNAP2*-rs114360492 (r^2 = 0), previously reported in GWAS of AD by proxy [17]. See results in Supplementary Results (Supplementary Figs. 5 and 6; Supplementary Table 5).

3.2. Genetic exploration of GR@ACE clinical endophenotypes and enrichment analysis

To explore whether clinical AD subgroups, representing GR@ACE endophenotypes, reflected variations in the underlying biological pathways driving dementia, we classified LOAD genetic variants into three categories. Category A comprised variants strongly related to the purest form of clinical AD (i.e., subjects with probable AD in primary and secondary diagnoses). The most prominent locus of this category was *APOE*-rs429358 (AD^{+++} OR = 2.92 [2.60–3.27], P value = 9.26 × 10^{-75}; VaD^{++} OR [95% confidence interval] = 1.27 [1.02–1.59], P value = .04). Other loci included in category A were *CR1*, *BIN1*, *MEF2C*, *MS4A2*, *PICALM*, *MAPT*, and *CD33*. In contrast, category B comprised variants with the strongest effect observed in subjects with AD mixed with vascular disease (*SORL1*, *ADAM10*, *CASS4*, *ATP5H*, and *ACE*) (Supplementary Table 1). Further description is provided in Supplementary Results. Category C comprised a group of variants with effects in all clinical endophenotypes (Fig. 2). Subanalysis for category C is shown in Supplementary Results and Supplementary Table 6.

Next, we explored biological pathways for each gene category. Note that the regulation of vasculature development and blood vessel morphogenesis were only detected for genes in category A, which is more closely related to

Table 2
Association results for lead single-nucleotide polymorphisms reaching genome-wide significance

Marker	Near locus	Position Chr:bp	A1/A2	MAF	Discovery stage	Stage I OR (95% CI)	P	Stage II (replica) OR (95% CI)	P	Stage I + II OR (95% CI)	P
rs117834366*	CNTNAP2	7:147634891	A/G	0.011	GR@ACE VaD^{++}	6.03 (3.22–11.2)	1.91×10^{-8}	1.09 (0.66–1.78)	.73	2.08 (1.42–3.07)	1.79×10^{-4}
rs4704171[†]	ANKRD31	5:74368254	C/T	0.123	GR@ACE + dbGaP	1.19 (1.12–1.27)	2.78×10^{-8}	1.10 (0.98–1.25)	.09	1.18 (1.11–1.24)	1.15×10^{-8}
rs10098778[†]	TP53INP1/NDUFAF6	8:95992020	C/T	0.470	GR@ACE + IGAP I & II	0.94 (0.91–0.96)	2.54×10^{-8}	0.96 (0.89–1.05)	.40	0.94 (0.92–0.96)	2.32×10^{-8}
rs7225151[†]	SCIMP	17:5137047	A/G	0.126	GR@ACE + IGAP I & II	1.10 (1.06–1.14)	8.98×10^{-8}	1.14 (1.00–1.30)	.04	1.10 (1.06–1.14)	1.38×10^{-8}
rs7225151[†]	SCIMP	17:5137047	A/G	0.126	GR@ACE AD^{+++} + IGAP I & II	1.11 (1.07–1.15)	1.12×10^{-8}	1.07 (0.88–1.30)	.49	1.11 (1.07–1.15)	9.45×10^{-9}

NOTE. The threshold for genome-wide significance was 5×10^{-8}. Position = GRCh37/hg19 coordinates Stage I corresponds to the discovery stage; stage II corresponds to the replica; stage I + II corresponds to the meta-analysis of GR@ACE VaD^{++} and the entire replica (N = 4959).

Abbreviations: AD, Alzheimer's disease; VaD, vascular dementia; chr:bp, chromosome:base pair; A1, minor allele; A2, mayor allele; MAF, minor allele frequency obtained from the GR@ACE study (N = 7409); OR, odds ratio; CI, confidence interval.

*Imputed variant; rs117834366 r2 = 0.68.
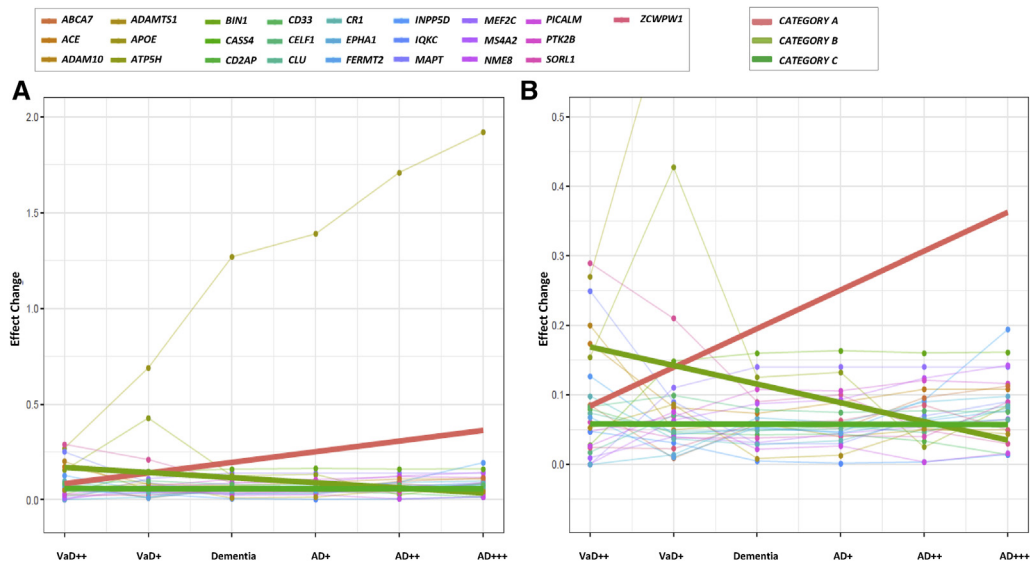
[†]Genotyped variant.

Fig. 2. (A) Enrichment trend per genetic marker and gene category across GR@ACE endophenotypes. (B) Graph centered in effect change range 0–0.5. Effect change per endophenotype = Variant Odds ratio–variant null effect; Enrichment trend per category was obtained applying a linear regression using ggplot2 in R. Abbreviations: AD, Alzheimer's disease; VaD, vascular dementia.

pure AD ($P = 2.03 \times 10^{-7}$, $P = 1.90 \times 10^{-6}$, respectively) (Table 3). Additional categories indicated immune system pathways (category B, $P = 2.07 \times 10^{-7}$; category C, $P = 5.77 \times 10^{-15}$) (Table 3). Finally, with the aim of validating previous results, we conducted a subanalysis by classifying LOAD genetic variants with more stringent classification criteria (Supplementary Methods). Again, *APOE*, *CR1*, *MEF2C*, *MS4A2*, and *PICALM* loci were found in category A; *SORL1* and *CASS4* were in category B; and additional AD loci were in category C (Supplementary Fig. 4). Regulation of vasculature development was exclusively identified as the top pathway in category A ($P = 2.14 \times 10^{-7}$) when we restricted the analysis to include those loci coexpressing with at least 4 LOAD genes (Supplementary Table 7). Further replication in cohorts with available neuropathological data would be recommended.

3.3. Meta-analysis of GR@ACE study with other data sets

To assess the impact of sample composition in AD GWAS, and look for new AD loci, we first combined the GR@ACE data set with nine additional genomic databases that had genotypic level data available. Subtle genomic inflation was detected, mainly explained by polygenicity ($\lambda_{GC} = 1.10$; LD score intercept = 1.04). Five regions were associated with LOAD (Fig. 3); of these, four (*APOE*-rs429358, *PICALM*-rs10792832, *MS4A2*-rs983392, and *BIN1*-rs6733839) have been previously linked to AD (Supplementary Table 8), and one is a new GWAS finding (*ANKDR31*-rs4704171; OR = 1.19 [1.12–1.27]; $P = 2.78 \times 10^{-8}$) (Table 2).

Then, we conducted a genome-wide meta-analysis combining the GR@ACE study with IGAP stage I. We

identified 12 LOAD genomic regions reaching GWS. *CD33*-rs3865444, which did not reach GWS in the IGAP meta-analysis, was significantly associated with LOAD (OR = 0.92 [0.89–0.95]; $P = 3.61 \times 10^{-8}$) (Supplementary Fig. 7). Among the top suggestive signals, we detected *HBEGF*-rs4150233 (OR = 0.92 [0.90–0.95]; $P = 5.10 \times 10^{-8}$) previously identified by a transethnic GWAS [29].

Next, meta-analysis of the whole GR@ACE data set with IGAP I and II enabled the identification, for the first time, of *NDUFAF6*-rs10098778 as a GWS signal (OR = 0.94 [0.91–0.96]; $P = 2.54 \times 10^{-8}$). When we combined GR@ACE AD^{+++} endophenotype with IGAP I and II, we also detected *SCIMP*-rs7225151 (OR = 1.11 [1.07–1.15]; $P = 1.12 \times 10^{-8}$) (Table 2) (Supplementary Fig. 8). It was previously reported as a genome-wide suggestive signal by IGAP [24]. Recently, *SCIMP*-rs113260531, which is in complete LD with our lead marker ($r^2 = 1$), was associated with AD [17].

3.4. Replication of genome-wide significant findings

Finally, we tested for replication of the new signals in an independent sample of 4959 Spanish individuals. The *CNTNAP2*-rs117834366, detected in the GWAS of GR@ACE VaD^{++} endophenotype, had a P value of 0.79 with a similar effect direction to that reported previously but strongly deflated in the entire replica sample (OR = 1.09 [0.66–1.78]; $P = .79$) (Table 3). Analysis of the subspecific VaD phenotype in the replica (N = 89) would be highly inaccurate.

In the exploration of meta-GWAS findings, we observed that the *ANKDR31*-rs4704171-C marker increased the risk of AD (OR = 1.10 [0.98–1.25]; $P = .09$; power = 33%).

Table 3
Top ten biological pathways per gene category

Gene ontology pathway	Top 10 coregulated pathways for category A	P value
GO:1901342	Regulation of vasculature development	2.03×10^{-7}
GO:0060326	Cell chemotaxis	2.59×10^{-7}
GO:0048771	Tissue remodeling	6.77×10^{-7}
GO:0050865	Regulation of cell activation	1.14×10^{-6}
GO:0007159	Leukocyte cell-cell adhesion	1.21×10^{-6}
GO:0048514	Blood vessel morphogenesis	1.90×10^{-6}
GO:0003012	Muscle system process	2.54×10^{-6}
GO:0002764	Immune response-regulating signaling pathway	3.48×10^{-6}
GO:0032103	Positive regulation of response to external stimulus	3.91×10^{-6}
GO:0010959	Regulation of metal ion transport	4.36×10^{-6}

Gene ontology pathway	Top 10 coregulated pathways for category B	P value
GO:0009620	Response to fungus	2.02×10^{-7}
GO:0050886	Endocrine process	3.58×10^{-7}
GO:0002443	Leukocyte mediated immunity	5.47×10^{-7}
GO:0050865	Regulation of cell activation	1.52×10^{-5}
GO:0031349	Positive regulation of defense response	8.42×10^{-5}
GO:0032103	Positive regulation of response to external stimulus	1.00×10^{-4}
GO:0002250	Adaptive immune response	1.30×10^{-4}
GO:0098542	Defense response to other organism	2.00×10^{-4}
GO:1901568	Fatty acid derivative metabolic process	2.24×10^{-4}
GO:0050900	Leukocyte migration	2.57×10^{-4}

Gene ontology pathway	Top 10 coregulated pathways for category C	P value
GO:0007159	Leukocyte cell-cell adhesion	5.77×10^{-15}
GO:0050865	Regulation of cell activation	4.37×10^{-14}
GO:0002764	Immune response-regulating signaling pathway	1.33×10^{-12}
GO:0002253	Activation of immune response	3.96×10^{-12}
GO:0002443	Leukocyte mediated immunity	4.34×10^{-12}
GO:0002274	Myeloid leukocyte activation	7.78×10^{-12}
GO:0002250	Adaptive immune response	1.24×10^{-11}
GO:0002263	Cell activation involved in immune response	7.07×10^{-11}
GO:0022407	Regulation of cell-cell adhesion	5.40×10^{-9}
GO:0070661	Leukocyte proliferation	1.22×10^{-8}

Although the expected effect is in line with previous data, the precision of the estimate in this replica differs, ranging from a 2% decrease (a small negative association) to a 25% increase. Of note, the result emerging from the meta-analysis of the replica with the discovery sample (n = 26,194) is compatible with its potential role in dementia (OR = 1.18 [1.11–1.24]; $P = 1.15 \times 10^{-8}$) (Table 3). See forest plot in Supplementary Fig. 9.

We observed a similar effect direction in the *NDUFAF6*-rs10098778 marker to that reported in the discovery stage, with interval estimates ranging from a risk decrease of 11% to a risk increase of 5% (OR = 0.96 [0.89–1.05]; $P = .40$; power = 16%). This signal had a $P = 2.32 \times 10^{-8}$ in the final meta-analysis, including the whole GR@ACE data set, the replica, and IGAP I and II (n = 91,373) (Supplementary Fig. 9).

SCIMP-rs7225151 showed a risk effect in the whole replica. Limits of the interval were consistent with a positive association (OR = 1.14 [1.01–1.29]; $P = .047$; power = 39%; n cases = 1943). In the AD^{+++} endophenotype, the marker presented the same positive risk effect direction (OR = 1.07 [0.88–1.30]), although had $P = .49$, which could be mainly explained by a reduction of the sample size (power = 19%; n cases = 584). Our results for both meta-analyses, the final meta-analysis of the whole GR@ACE data set (n = 91,373) and the final meta-analysis of GR@ACE AD^{+++} endophenotype, (n = 85,055) were compatible with a potential effect of this marker in AD (Table 3). See forest plots in Supplementary Fig. 9.

3.5. Biological interpretation of meta-GWAS signals

To identify candidate genes and potential causal variants within novel meta-GWAS regions, we conducted cis-eQTL mapping. The rs2335107 marker located in the *ANKRD31* locus (chr5:74,451,693) was associated with the cortical expression of the long noncoding RNA (lncRNA) CTD-2235C13.3 ($P = 1.26 \times 10^{-5}$). This variant is located 83.4 kb from the meta-GWAS lead single nucleotide polymorphism (rs4704171, chr5:74,368,254), and both are in complete LD ($r^2 = 1$). The *CTD-2235C13.3* gene is located 1.6 kb from the *HMGCR* locus, and its function is unknown. The *NDUFAF6* region mapped for NDUFAF6 RNA cortical expression ($P = 5.56 \times 10^{-6}$) and for TP53INP1 RNA blood expression ($P = 1.17 \times 10^{-10}$). Finally, rs73976325 (chr17:5,123,227), located in the *SCIMP* locus, to 13.8 kb from the meta-GWAS top signal (rs7225151, chr17:5,137,047), mapped to brain cis-acting eQTL for AC012146.1 lincRNA ($P = 2.15 \times 10^{-7}$). Two additional markers were pinpointed to blood eQTLs, *SCIMP*-rs6502851 ($P = 3.89 \times 10^{-08}$) and *RABEP*-rs59277121 ($P = 3.89 \times 10^{-8}$) (Supplementary Table 3). In an additional prioritization strategy, combining information from positional mapping, eQTL, chromatin interaction, and gene-based genome-wide association analysis via FUMA, results pointed to *ANKDR31* and *POLK* for the *ANKDR31* genomic region, as well as *NDUFAF6* and *TP53INP*1 for the *NDUFAF6* region (Supplementary Table 9). Further description is provided in Supplementary Information and Supplementary Table 9.

4. Discussion

We present a comprehensive GWAS of AD dementia cases. This represents the first pilot study exploring the genetics and underlying biological pathways of subgroups of patients with AD, defined based on vascular burden. We
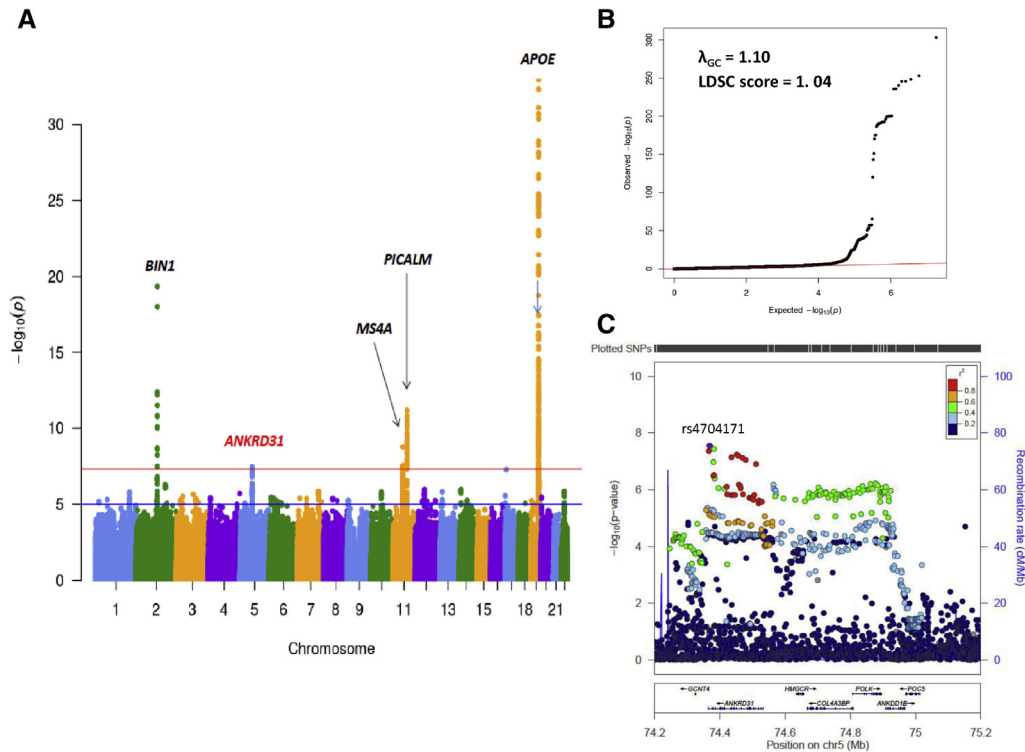
Fig. 3. A) Results of genome-wide association analysis for GR@ACE meta-analysis with nine additional databases (n = 21,235). (B) QQplot. (C) Associations of the region centered on rs4704171 located in the *ANKRD31* locus and containing the *HMGCR* locus.

showed differential biological routes underlying clinical endophenotypes and demonstrated how these differential subgroups of patients with AD impact GWAS discoveries. The GR@ACE study represents a unique genomic resource because all affected cases were diagnosed in a single memory clinic using the same screening and diagnostic techniques. This might limit potential sources of clinical variation between study participants, recently demonstrated in a large meta-GWAS [12].

Based on the increase in evidence suggesting that vascular brain pathology can act concomitantly with AD to produce a more rapid cognitive decline [5], we explored the effect of known LOAD loci across different levels of vascular burden in dementia patients using only clinical definitions. Our basic idea was to dissect, from a molecular point of view, the model previously proposed by Viswanathan et al. [7]. We observed three categories of loci, which might reflect the disease's clinical heterogeneity, from vascular and mixed forms to a "purer" AD phenotype. Intriguingly, we detected vascular processes to be the main causal mechanism in clinically pure AD and found the immune system pervasively detected across the three categories. Although both pathways have been previously associated with LOAD by network analysis [30], this is the first study to show that the association with the vascular system is conducted by AD-specific clinical subgroup.

It should be noted that the present study used clinical criteria to define the AD cases [20], but recently the classification of AD has evolved. In 2018, the NIA-AA proposed a novel research framework for the biological classification of AD based on the presence *in vivo* of biomarker evidences for amyloid (A), tau (T), and neurodegeneration (N), as surrogate of the neuropathological state of an individual [31]. The AT(N) biomarker system allows the classification of individuals into three categories: those with a normal biomarker profile, those with biomarkers compatible with AD change, and those with biomarkers compatible with non-AD pathological changes [31]. Using the NIA-AA approach, the generation of subgroups of AD patients considering vascular pathology would be unfeasible, as nowadays the ATN classification does not integrate measures of vascular dysfunction. Taking into account that most of dementia cases are caused by mixed pathologies, the current system seems deeply incomplete to study the probable interaction between neurodegeneration and vascular dysfunction. This idea has also been claimed by others [32,33]. Thus, we encourage other groups to contrast the proposed loci classification, which was based on the GR@ACE clinical endophenotypes, but using well-powered GWAS cohorts with available neuropathological data.

Silent changes occur in brain microvasculature during AD progression. In fact, CAA is a well-recognized AD pathological feature characterized by the accumulation of amyloid proteins in the walls of small cerebral vessels. CAA has been proposed to compromise the perivascular drainage

of Aβ from the brain to the peripheral system [34]. Almost all AD brains harbor CAA pathology to some extent, although *in vivo* most CAA cases remain undiagnosed, even using the validated Boston criteria [35]. Mendelian mutations of the *APP* gene have been found in CAA and AD [8,36]. *APOE* ε4 and *CR1* have been associated with an increased risk of CAA [37,38]. In particular, distinct AD loci have been associated with capillary and noncapillary CAA [39]. Between them, *APOE* ε4 was strongly related to capillary CAA [39]. These links make it conceivable that a potential genetic overlap exists between CAA and AD and suggest that CAA pathology could represents an underlying process for AD. In that context, we think that intrinsic alterations to the vasculature could contribute to disease pathogenesis in more pure forms of AD, explaining our results. Conversely, in AD individuals with evident cerebrovascular lesions comprising mixed forms, the additional role of cardiovascular risk factors such as hypertension, atherosclerosis, or arteriosclerosis should be considered, as these could point to a systemic pathological state leading to vascular damage and dementia. This would agree with the limited genetic correlation between neurodegenerative and other neurologic disorders [12], as well as with the results obtained from heterochronic parabionts in aging models [40].

Understanding the role of vasculature pathology in AD seems to be a pertinent step. In that scenario, CAA would be a key AD hallmark. CAA represents the unique identified link between the vascular and amyloid hypotheses, but it has been completely neglected in the original hypothesis formulation.

From a clinical point of view, placing each patient somewhere along the disease spectrum proposed by Viswanathan et al. [7] is complex. A deep understanding of heterogeneity in AD seems necessary to design better genetic studies, which must drive the discovery of novel loci and, ultimately, innovative targets for AD therapies. In this study, we explored how clinical heterogeneity might impact GWAS findings by integrating distinct GWAS data sets with either the GR@ACE cohort as a whole or its endophenotypes. We found several new GWS signals that seem strongly dependent on the sample composition. For example, after combining IGAP stages I and II with the entire GR@ACE data set, we identified genetic signals in the *NDUFAF6* genomic region but not in the *SCIMP* region. When this exercise was conducted using GR@ACE endophenotypes, the *SCIMP* signal was detected using the clinically "pure" AD GR@ACE endophenotype. It should be noted that the power to detect *SCIMP* signal in the meta-analysis with GRA@ACE dementia and GR@ACE AD[+++] was 75 and 70%, respectively. We tried to replicate this finding in a purer AD data set without clinical mixed dementia cases, but the available number of clinical AD[+++] cases might be compromising the statistical power to replicate (N cases = 584; power = 19%). Despite that, we think that using specific clinical subgroups of the AD population might empower genetic studies to detect genes associated with specific disease axes.

An alternative strategy is taking advantage of clinical heterogeneity. Specifically, heterogeneity might play a dual role in genetic studies. Although it might decrease the power to detect genes associated with more specific clinical subgroups, incorporating detailed clinical AD definitions can also promote identifying genes shared with other conditions or copathologies such as small vessel disease (SVD). In fact, this was the case for the *ATP5H* locus, which was previously found to be associated with AD [41] and more recently found in relation to SVD [42]. We think that the same could apply to the *ANKRD31* finding. *ANKRD31* encodes a protein containing ankyrin repeats, which is linked with neurodevelopmental disorders [43]. Of note, *ANKRD31* GWAS signal mapped to the brain eQTL of a lncRNA, located 1.6 kb from the *HMGCR* locus and residing in the *COL4A3BP* gene. The *HMGCR* locus is one of the most important coregulators of cholesterol biosynthesis, and it is the therapeutic target of statins. The *COL4A3BP* gene is involved in lipid transport [44]. Several studies have linked *HMGCR* polymorphisms and AD risk or age at onset for AD [45], and the cholesterol pathway has been identified to be a biological route shared between AD and SVD. Interestingly, markers in the *POLK* locus, associated by gene-based genome-wide association analysis on this study and located in the same disequilibrium block of *ANKDR31* (Fig. 3), jointly conferred risk for AD and plasma levels of LDL [46]. Considering prior findings, our results are consistent with this genomic region having a role in mixed dementia. The reported genetic signal should be considered a highly probable finding, although independent replications are still required.

In the present work, *NDUFAF6* signals reached GWS for the first time. This finding presented the same effect direction in the independent sample (power = 16%) and remains as GWS after the final meta-analysis. Our lead GWAS marker is in high LD with *NDUFAF6*-rs4735340, the top suggestive signal reported by Kunkle et al. [18] at this region ($r^2 = 0.95$, for Utah residents of European ancestry population). Despite that, there are subtle differences in LD estimates for the Iberian population ($r^2 = 0.87$), suggesting that the genetic architecture of the Spanish population could be helping to pinpoint the region of interest. This region is in the close vicinity of *TP53INP1*, previously associated with AD by a gene-based approach [47]. *TP53INP1* is involved in mitochondrial function. Considering these findings and results emerging from eQTL analysis, it would be feasible that a regulatory element for *NUDFAF6* resides upstream of the *TP53INP1* locus. We also detected that the *SCIMP* signal was mainly conducted by a specific group of AD cases. This signal was reported to be a suggestive signal by IGAP [24], and a proxy of it (*SCIMP*-rs113260531) reached GWS recently [17]. *SCIMP* regions has been involved in several eQTLs, from uncharacterized cortical lncRNA to blood eQTLs in *SCIMP* and *RABEP1* loci, both

associated with immune system function [48,49]. The *CD33* locus remains a controversial LOAD locus because large meta-GWAS were unable to replicate this signal [24], but here it reached GWS. We previously proposed that cryptic population substructure could explain the divergent observations for this locus [50].

Note that the lack of definitive neuropathological data for AD cases is a severe limitation of the present study. Clinical definitions have important uncertainties, and diagnosis misclassifications sometimes occur. Hence, some AD individuals included in enriched AD endophenotypes may present concomitant vascular brain disease. The generation of large histopathological GWAS cohorts with associated quantitative data on each pathological hallmark is the ultimate solution to tackling the intrinsic heterogeneity in AD. Unfortunately, there are few examples of neuropathological cohorts: only one GWAS has investigated the genetics of CAA, with *APOE* being the unique GWS signal [37]. In this study, a small number of AD cases evolved to vascular dementia during follow-up. Large cross-sectional clinical GWAS cannot control diagnostic changes occurring in clinical practice. Clinical diagnosis is a dynamic variable, so understanding the genetic profiles of subgroups of patients evolving to other pathologies would provide powerful information.

It should be considered that there is a limitation in reducing the sample size by splitting the cohort into different endodophenotypes, instead of combining them. Despite that, spanning the spectrum of dementia individuals to generate clinical endophenotypes provided us a versatile design, which let us explore the effect of heterogeneity in GWAS and replicate the main findings of pathway analysis using an alternative strategy. The limited number of VaD cases in subgroup analysis limits the accuracy of gene categorization and pathway analysis. Finally, the exact effector genes for LOAD genetic findings remain unclear. This is a severe limitation to pathway analysis that can only be circumvented by isolating the causative mutations. Independent replication will be needed to corroborate our new GWS signals. In that sense, the selection of specific patient groups might lead to successful replication studies.

The assessment of heterogeneity has important implications for gene discovery, the development of treatments, and their appropriate use in individual patients. The GR@ACE cohort provides useful genomic information, as it accounts for potential sources of variability and contains different subgroups of cases. This enabled us to analyze the LOAD genetic landscape in terms of clinical endophenotypes. Our efforts to disentangle the mechanistic pathways operating under clinical subgroups of patients revealed that vasculature regulation may be an essential part of the causative mechanism of LOAD. Finally, our exploration of AD genetics highlights the relevance of sample composition in genetic discoveries. Considering sample composition in the design of genetic studies might lead to the identification of genetic profiles, which can help clinicians distinguish subsets of patients within the disease spectrum and promote novel therapy targets for AD.

The GR@ACE study group: Abdelnour C[1,2], Aguilera N[1], Alarcon E[1,3], Alegret M[1,2], Benaque A[1], Boada M[1,2], Buendia M[1], Cañabate P[1,2], Carracedo A[4,5], Corbatón A[6], de Rojas I[1], Diego S[1], Espinosa A[1,2], Gailhajenet A[1], García González P[1], Gil S[1], Guitart M[1], González Pérez A[7], Hernández I[1,2], Ibarria, M[1], Lafuente A[1], Macias J[8], Maroñas O[4], Martín E[1], Martínez MT[6], Marquié M[1], Mauleón A[1], Monté-Rubio G[1], Montrreal L[1], Moreno-Grau S[1,2], Moreno M[1], Orellana A[1], Ortega G[1,2], Pancho

A[1], Pelejà E[1], Pérez-Cordon A[1], Pineda JA[8], Preckler S[1], Quintela I[3], Real LM[3,8], Rodríguez-Gómez O[1,2], Rosende-Roca M[1], Ruiz A[1,2], Ruiz S[1,2], Sáez ME[7], Sanabria A[1,2], Santos-Santos MA[1], Serrano-Rios M[6], Sotolongo-Grau O[1], Tárraga L[1,2], Valero S[1,2], Vargas L[1] (1. Research Center and Memory clinic Fundació ACE. Institut Català de Neurociències Aplicades. Universitat Internacional de Catalunya. Barcelona, Spain; 2. CIBERNED, Center for Networked Biomedical Research on Neurodegenerative Diseases, National Institute of Health Carlos III, Ministry of Economy and Competitiveness, Spain; 3. Dep. of Surgery, Biochemistry and Molecular Biology, School of Medicine. University of Málaga. Málaga, Spain; 4. Grupo de Medicina Xenómica, Centro Nacional de Genotipado (CEGEN-PRB3-ISCIII). Universidade de Santiago de Compostela, Santiago de Compostela, Spain; 5. Fundación Pública Galega de Medicina Xenómica- CIBERER-IDIS, Santiago de Compostela, Spain; 6. Centro de Investigación Biomédica en Red de Diabetes y Enfermedades Metabólicas Asociadas, CIBERDEM, Spain, Hospital Clínico San Carlos, Madrid, Spain; 7. CAEBI. Centro Andaluz de Estudios Bioinformáticos., Sevilla, Spain; 8. Unidad Clínica de Enfermedades Infecciosas y Microbiología. Hospital Universitario de Valme, Sevilla, Spain)

DEGESCO consortium: Adarmes-Gómez AD[1,2], Alarcón-Martín E[3,4], Álvarez I[5], Álvarez V[6,7], Amer-Ferrer G[8], Antequera M[9], Antúnez C[9], Baquero M[10], Bernal M[11], Blesa R[2,12], Boada M[2,3], Buiza-Rueda D[1,2], Bullido MJ[2,13,14], Burguera JA[10], Calero M[2,15,16], Carrillo F[1,2], Carrión-Claro M[1,2], Casajeros MJ[17], Clarimón J[2,12], Cruz-Gamero JM[4], de Pancorbo MM[18], de Rojas I[3], del Ser T[14], Diez-Fairen M[5], Fortea J[2,12], Franco E[11], Frank-García A[2,14,19], García-Alberca JM[20], Garcia Madrona S[16], Garcia-Ribas G[16], Gómez-Garre P[1,2], Hernández I[2,3], Hevilla S[20], Jesús S[1,2], Labrador Espinosa MA[1,2], Lage C[2,21], Legaz A[9], Lleó A[2,12], López de Munáin A[22], López-García S[2,21], Macias D[1,2], Manzanares S[9,23], Marín M[11], Marín-Muñoz J[9], Marín T[20], Marquié M[3], Martín Montes A[2,13,19], Martínez B[9], Martínez C[7,24], Martínez V[9], Martínez-Lage Álvarez P[25], Medina M[2,14], Mendioroz Iriarte M[26], Menéndez-González M[7,27], Mir P[1,2], Molinuevo JL[28], Monté-Rubio G[3], Montrreal L[3], Moreno-Grau S[2,3], Orellana A[3], Pastor AB[15], Pastor P[5], Pérez Tur J[2,29,30], Periñán-Tocino T[1,2], Piñol Ripoll G[2,31], Rábano A[2,15,32], Real de Asúa D[33], Rodrigo S[11], Rodríguez-Rodríguez E[2,21], Royo JL[4], Ruiz A[2,3], Sanchez del Valle Díaz R[34], Sánchez-Juan P[2,21], Sastre I[2,13], Sotolongo-Grau O3, Tárraga L[2,3], Valero S[2,3], Vicente MP[9], Vivancos L[9] (1. Unidad de Trastornos del Movimiento, Servicio de Neurología y Neurofisiología. Instituto de Biomedicina de Sevilla (IBiS), Hospital Universitario Virgen del Rocío/CSIC/Universidad de Sevilla, Seville, Spain; 2. CIBERNED, Network Center for Biomedical Research in Neurodegenerative Diseases, National Institute of Health Carlos III, Spain; 3. Research Center and Memory clinic Fundació ACE. Institut Català de Neurociències Aplicades. Universitat Internacional de Catalunya. Barcelona, Spain; 4. Dep. of Surgery, Biochemistry and Molecular Biology, School of Medicine. University of Málaga. Málaga, Spain; 5. Fundació per la Recerca Biomèdica i Social Mútua Terrassa, and Memory Disorders Unit, Department of Neurology, Hospital Universitari Mutua de Terrassa, University of Barcelona School of Medicine, Terrassa, Barcelona, Spain; 6. Laboratorio de Genética Hospital Universitario Central de Asturias, Oviedo; 7. Instituto de Investigación Biosanitaria del Principado de Asturias (ISPA); 8. Department of Neurology, Hospital Universitario Son Espases, Palma, Spain; 9. Unidad de Demencias. Hospital Clínico Universitario Virgen de la Arrixaca; 10. Servei de Neurologia, Hospital Universitari i Politècnic La Fe; 11. Unidad de Demencias, Servicio de Neurología y Neurofisiología. Instituto de Biomedicina de Sevilla (IBiS), Hospital Universitario Virgen del Rocío/CSIC/Universidad de Sevilla, Seville, Spain; 12. Memory Unit, Neurology Department and Sant Pau Biomedical Research Institute, Hospital de la Santa Creu i Sant Pau, Universitat Autònoma de Barcelona, Barcelona, Spain; 13. Centro de Biologia Molecular Severo Ochoa (C.S.I.C.-U.A.M.), Universidad Autonoma de Madrid, Madrid, Spain; 14. Instituto de Investigacion Sanitaria 'Hospital la Paz' (IdIPaz), Madrid, Spain; 15. CIEN Foundation, Queen Sofia Foundation Alzheimer Center, Madrid, Spain; 16. Instituto de Salud Carlos III (IS-CIII), Madrid, Spain; 17. Hospital Universitario Ramón y Cajal; Madrid, Spain; 18. BIOMICs, País Vasco; Centro de Investigación Lascaray. Universidad del País Vasco UPV/EHU; 19. Neurology Service, Hospital Universitario La Paz (UAM), Madrid, Spain; 20. Alzheimer Research Center & Memory Clinic. Andalusian Institute for Neuroscience. Málaga, Spain; 21. Neurology Service, Marqués de Valdecilla University Hospital (University of Cantabria and IDIVAL), Santander, Spain; 22. Hospital Donostia de San Sebastián; 23. Fundación para la Formación e Investigación Sanitarias de la Región de Murcia; 24. Servicio de Neurología -Hospital de Cabueñes-Gijón; 25. Centro de Investigación y Terapias Avanzadas. Fundación CITA-alzheimer; 26. Navarrabiomed; 27. Servicio de Neurología -Hospital Universitario Central de Asturias, Oviedo; 28. Barcelona βeta Brain Research Center – Fundació Pasqual Maragall; 29. Unitat de Genètica Molecular. Institut de Biomedicina de València-CSIC; 30. Unidad Mixta de Neurologia Genètica. Instituto de Investigación Sanitaria La Fe; 31. Unitat Trastorns Cognitius, Hospital Universitari Santa Maria de Lleida, Institut de Recerca Biomédica de Lleida (IRBLLeida), Lleida, España. 32. BT-CIEN; 33. Hospital Universitario La Princesa, Madrid, Spain; 34. Hospital Clínic Barcelona).

Supplementary Data

Supplementary data related to this article can be found at https://doi.org/10.1016/j.jalz.2019.06.4950.

References

[1] Baumgart M, Snyder HM, Carrillo MC, Fazio S, Kim H, Johns H. Summary of the evidence on modifiable risk factors for cognitive decline and dementia: a population-based perspective. Alzheimers Dement 2015;11:718–26.

[2] Brookmeyer R, Johnson E, Ziegler-Graham K, Arrighi HM. Forecasting the global burden of Alzheimer's disease. Alzheimers Dement 2007;3:186–91.

[3] Toledo JB, Arnold SE, Raible K, Brettschneider J, Xie SX, Grossman M, et al. Contribution of cerebrovascular disease in autopsy confirmed neurodegenerative disease cases in the National Alzheimer's Coordinating Centre. Brain 2013;136:2697–706.

[4] Serrano-Pozo A, Frosch MP, Masliah E, Hyman BT. Neuropathological Alterations in Alzheimer Disease. Cold Spring Harb Perspect Med 2011;1:a006189.

[5] Regan C, Katona C, Walker Z, Hooper J, Donovan J, Livingston G. Relationship of vascular risk to the progression of Alzheimer disease. Neurology 2006;67:1357–62.

[6] Arvanitakis Z, Capuano AW, Leurgans SE, Bennett DA, Schneider JA. Relation of cerebral vessel disease to Alzheimer's disease dementia and cognitive function in elderly people: a cross-sectional study. Lancet Neurol 2016;15:934–43.

[7] Viswanathan A, Rocca WA, Tzourio C. Vascular risk factors and dementia: how to move forward? Neurology 2009;72:368–74.

[8] Goate A, Chartier-Harlin MC, Mullan M, Brown J, Crawford F, Fidani L, et al. Segregation of a missense mutation in the amyloid precursor protein gene with familial Alzheimer's disease. Nature 1991; 349:704–6.

[9] Sherrington R, Rogaev EI, Liang Y, Rogaeva EA, Levesque G, Ikeda M, et al. Cloning of a gene bearing missense mutations in early-onset familial Alzheimer's disease. Nature 1995; 375:754–60.

[10] Sherrington R, Froelich S, Sorbi S, Campion D, Chi H, Rogaeva EA, et al. Alzheimer's disease associated with mutations in presenilin 2 is rare and variably penetrant. Hum Mol Genet 1996;5:985–8.

[11] Hardy JA, Higgins GA. Alzheimer's disease: the amyloid cascade hypothesis. Science 1992;256:184–5.

[12] Brainstorm Consortium V, Anttila V, Bulik-Sullivan B, Finucane HK, Walters RK, Bras J, et al. Analysis of shared heritability in common disorders of the brain. Science 2018;360:eaap8757.

[13] Avramopoulos D. Genetics of Alzheimer's disease: recent advances. Genome Med 2009;1:34.

[14] Corder E, Saunders A. Gene dose of apolipoprotein E type 4 allele and the risk of Alzheimer's disease in late onset families. Science 1993; 8:41–3.

[15] Kunkle BW, Grenier-Boley B, Sims R, Bis JC, Naj AC, Boland A, et al. Meta-analysis of genetic association with diagnosed Alzheimer's disease identifies novel risk loci and implicates Abeta, Tau, immunity and lipid processing. BioRxiv 2018:294629.

[16] Sims R, van der Lee SJ, Naj AC, Bellenguez C, Badarinarayan N, Jakobsdottir J, et al. Rare coding variants in PLCG2, ABI3, and TREM2 implicate microglial-mediated innate immunity in Alzheimer's disease. Nat Genet 2017;49:1373–84.

[17] Jansen IE, Savage JE, Watanabe K, Bryois J, Williams DM, Steinberg S, et al. Genome-wide meta-analysis identifies new loci and functional pathways influencing Alzheimer's disease risk. Nat Genet 2019;51:404–13.

[18] Kunkle BW, Grenier-Boley B, Sims R, Bis JC, Damotte V, Naj AC, et al. Genetic meta-analysis of diagnosed Alzheimer's disease identifies new risk loci and implicates Aβ, tau, immunity and lipid processing. Nat Genet 2019;51:414–30.

[19] Ridge PG, Hoyt KB, Boehme K, Mukherjee S, Crane PK, Haines JL, et al. Assessment of the genetic variance of late-onset Alzheimer's disease. Neurobiol Aging 2016;41:200.e13–200.e20.

[20] McKhann GM, Knopman DS, Chertkow H, Hyman BT, Jack CR, Kawas CH, et al. The diagnosis of dementia due to Alzheimer's disease: recommendations from the National Institute on Aging-Alzheimer's Association workgroups on diagnostic guidelines for Alzheimer's disease. Alzheimers Dement 2011;7:263–9.

[21] Boada M, Tárraga L, Hernández I, Valero S, Alegret M, Ruiz A, et al. Design of a comprehensive Alzheimer's disease clinic and research center in Spain to meet critical patient and family needs. Alzheimers Dement 2014;10:409–15.

[22] Román GC, Tatemichi TK, Erkinjuntti T, Cummings JL, Masdeu JC, Garcia JH, et al. Vascular dementia: diagnostic criteria for research studies. Report of the NINDS-AIREN International Workshop. Neurology 1993;43:250–60.

[23] Gauderman WJ. Sample size requirements for matched case-control studies of gene-environment interaction. Stat Med 2002;21:35–50.

[24] Lambert JC, Ibrahim-Verbaas CA, Harold D, Naj AC, Sims R, Bellenguez C, et al. Meta-analysis of 74,046 individuals identifies 11 new susceptibility loci for Alzheimer's disease. Nat Genet 2013; 45:1452–8.

[25] Wasserstein RL, Lazar NA. The ASA's statement on p-values: context, process, and purpose. Am Stat 2016;70:129–33.

[26] Wasserstein RL, Schirm AL, Lazar NA. Moving to a World Beyond "$p < 0.05$". Am Stat 2019;73:1–19.

[27] Machiela MJ, Chanock SJ. LDlink: a web-based application for exploring population-specific haplotype structure and linking correlated alleles of possible functional variants: Fig. 1. Bioinformatics 2015;31:3555–7.

[28] Watanabe K, Taskesen E, van Bochoven A, Posthuma D. Functional mapping and annotation of genetic associations with FUMA. Nat Commun 2017;8:1826.

[29] Jun GR, Chung J, Mez J, Barber R, Beecham GW, Bennett DA, et al. Transethnic genome-wide scan identifies novel Alzheimer's disease loci. Alzheimers Dement 2017;13:727–38.

[30] Zhang B, Gaiteri C, Bodea L-G, Wang Z, McElwee J, Podtelezhnikov AA, et al. Integrated systems approach identifies genetic nodes and networks in late-onset Alzheimer's disease. Cell 2013;153:707–20.

[31] Jack CR, Bennett DA, Blennow K, Carrillo MC, Dunn B, Haeberlein SB, et al. NIA-AA Research Framework: toward a biological definition of Alzheimer's disease. Alzheimers Dement 2018; 14:535–62.

[32] Sweeney MD, Montagne A, Sagare AP, Nation DA, Schneider LS, Chui HC, et al. Vascular dysfunction-The disregarded partner of Alzheimer's disease. Alzheimers Dement 2019;15:158–67.

[33] Hachinski V. Dementia: paradigm shifting into high gear. Alzheimers Dement 2019;15:985–94.

[34] Weller RO, Boche D, Nicoll JAR. Microvasculature changes and cerebral amyloid angiopathy in Alzheimer's disease and their potential impact on therapy. Acta Neuropathol 2009;118:87–102.

[35] Charidimou A, Shoamanesh A, Al-Shahi Salman R, Cordonnier C, Perry LA, Sheth KN, et al. Cerebral amyloid angiopathy, cerebral microbleeds and implications for anticoagulation decisions: the need for a balanced approach. Int J Stroke 2018;13:117–20.

[36] Sakai K, Yamada M. Cerebral amyloid angiopathy. Brain Nerve 2014; 66:827–35.

[37] Beecham GW, Hamilton K, Naj AC, Martin ER, Huentelman M, Myers AJ, et al. Genome-wide association meta-analysis of neuropathologic features of Alzheimer's disease and related dementias. PLoS Genet 2014;10:e1004606.

[38] Biffi A, Shulman JM, Jagiella JM, Cortellini L, Ayres AM, Schwab K, et al. Genetic variation at CR1 increases risk of cerebral amyloid angiopathy. Neurology 2012;78:334–41.

[39] Mäkelä M, Kaivola K, Valori M, Paetau A, Polvikoski T, Singleton AB, et al. Alzheimer risk loci and associated neuropathology in a population-based study (Vantaa 85+). Neurol Genet 2018;4:e211.

[40] Villeda SA, Plambeck KE, Middeldorp J, Castellano JM, Mosher KI, Luo J, et al. Young blood reverses age-related impairments in cognitive function and synaptic plasticity in mice. Nat Med 2014; 20:659–63.

[41] Boada M, Antúnez C, Ramírez-Lorca R, DeStefano A, González-Pérez A, Gayán J, et al. ATP5H/KCTD2 locus is associated with Alzheimer's disease risk. Mol Psychiatry 2014;19:682–7.

[42] Traylor M, Adib-Samii P, Harold D, Alzheimer's Disease Neuroimaging Initiative the ADN, International Stroke Genetics Consortium (ISGC), UK Young Lacunar Stroke DNA resource TISGC, Dichgans M, et al. Shared genetic contribution to Ischaemic Stroke and Alzheimer's Disease. Ann Neurol 2016; 79:739.

[43] Lucariello M, Vidal E, Vidal S, Saez M, Roa L, Huertas D, et al. Whole exome sequencing of Rett syndrome-like patients reveals the mutational diversity of the clinical phenotype. Hum Genet 2016; 135:1343–54.

[44] Hanada K, Kumagai K, Yasuda S, Miura Y, Kawano M, Fukasawa M, et al. Molecular machinery for non-vesicular trafficking of ceramide. Nature 2003;426:803–9.

[45] Leduc V, De Beaumont L, Théroux L, Dea D, Aisen P, Petersen RC, et al. HMGCR is a genetic modifier for risk, age of onset and MCI conversion to Alzheimer's disease in a three cohorts study. Mol Psychiatry 2015;20:867–73.

[46] Broce IJ, Tan CH, Fan CC, Jansen I, Savage JE, Witoelar A, et al. Dissecting the genetic relationship between cardiovascular risk factors and Alzheimer's disease. Acta Neuropathol 2019; 137:209–26.

[47] Escott-Price V, Bellenguez C, Wang L-S, Choi S-H, Harold D, Jones L, et al. Gene-wide analysis detects two new susceptibility genes for Alzheimer's disease. PLoS One 2014;9:e94661.

[48] Luo L, Bokil NJ, Wall AA, Kapetanovic R, Lansdaal NM, Marceline F, et al. SCIMP is a transmembrane non-TIR TLR adaptor that promotes proinflammatory cytokine production from macrophages. Nat Commun 2017;8:14133.

[49] Delunardo F, Margutti P, Pontecorvo S, Colasanti T, Conti F, Riganò R, et al. Screening of a microvascular endothelial cDNA library identifies rabaptin 5 as a novel autoantigen in Alzheimer's disease. J Neuroimmunol 2007;192:105–12.

[50] Moreno-Grau S, Hernández I, Heilmann-Heimbach S, Ruiz S, Rosende-Roca M, Mauleón A, et al. Genome-wide significant risk factors on chromosome 19 and the APOE locus. Oncotarget 2018; 9:24590–600.